Hindawi
International Transactions on Electrical Energy Systems
Volume 2022, Article ID 5076611, 17 pages
https://doi.org/10.1155/2022/5076611

*Research Article*

# Modified Fast Terminal Sliding Mode Control for DC-DC Buck Power Converter with Switching Frequency Regulation

**Güven Balta**,[1] **Naki Güler**,[2] **and Necmi Altin**[2]

[1]*Department of Electrical and Electronics Engineering, Faculty of Engineering and Architecture, Erzurum Technical University, Erzurum, Turkey*
[2]*Department of Electrical and Electronics Engineering, Faculty of Technology, Gazi University, Ankara, Turkey*

Correspondence should be addressed to Necmi Altin; naltin@gazi.edu.tr

Received 19 March 2022; Revised 22 September 2022; Accepted 14 October 2022; Published 31 October 2022

Academic Editor: Shaofeng Lu



In this paper, a modified fast terminal sliding mode control (FTSMC) with a fixed switching frequency is proposed for regulating the output voltage of the DC-DC buck converters. The design steps of the proposed FTSMC such as the selection of sliding surface, switching control strategy, existence, robustness, and stability analysis are presented in detail. To overcome the variable switching frequency in FTSMC, a frequency control loop is designed. Moreover, the proposed FTSMC with fixed switching frequency can be implemented by using only one voltage sensor. Hence, the proposed control method not only offers a fast dynamic response and fixed switching frequency but also simplifies the controller design in practical implementation. The effectiveness of the proposed control methods has been investigated by experimental studies. The results reveal that the proposed methods exhibit a good performance under both steady-state and dynamic transients caused by the variations in load resistance, input voltage, and reference voltage. Moreover, the proposed method is compared with four existing methods.

## 1. Introduction

The improvements in technology have caused massive developments in many fields such as industry, manufacturing, medical, communication, mechanics, energy, and military, over the past decade. Power converters are widely used almost in all of these fields. Therefore, the interest in power converters is increasing, day by day. On the other hand, power components have undergone a fast evolution. As a result of this evolution, some improvements are achieved in terms of cost, energy consumption, size, efficiency, and lifetime [1, 2]. These improvements are also reflected in electronic circuits which use power components. Hence, the size, cost, and weight of the power electronic systems are reduced while the efficiency is increased [3].

DC-DC converters are an example of powerful and sophisticated electronic circuits which is structured with the improved power components. Generally, DC-DC converters are utilized as a power supply in a similar fashion to the traditional linear power supplies. In comparison to linear alternatives, DC-DC converters have a lot of outstanding advantages such as stepping up/down, reversing the polarity of the output voltage, a higher efficiency, operating in a much larger DC input voltage range, the ability to operate in a wide input voltage range, [4, 5] lower power loss, smaller-size, and cost-effective structure [6]. All of these qualities are paving the way for DC-DC converters to become more widespread. Hence, they are used as replacements for the linear counterparts in many areas where higher efficiency and smaller size or lighter weight are required [7] such as personal computers, computer peripherals, communication, medical electronics, and adapters of consumer electronic devices [8].

There are various types of DC-DC converters that are derived from modifying the location of the advanced power components. The main types of DC-DC converters can be described as buck, boost, and buck-boost converters. These converters are used to convert DC input voltage at a certain level to obtain a regulated DC output voltage at a different level with very high conversion efficiency [6] for static and

dynamic loads [9]. Among them, the buck converter has drawn the attention of many researchers because it is the most popular in the industry as well as the most basic power converter due to its linear and minimum phase type by nature [10]. As a result of these characteristics, it has been extensively utilized in various kinds of applications where the required output voltage is lower than the input voltage, for instance, mobile phones, DC motor drives, computer systems, renewable energy systems, LED drivers [6, 11–13].

In general, buck converters are fed by an input voltage from a battery or other source, such as renewable energy, and then convert this voltage to the desired output voltage to use in a load. However, the desired output voltage may vary in steps, and even within a wide range in some applications [14]. This requires a good closed-loop mechanism so that the output voltage can track various desired reference voltage satisfactorily. Apart from the variation in reference voltage, unreliable input voltage, unanticipated load disturbances, and parametric and nonparametric uncertainties in the used model also give rise to poor dynamic response [15]. Hence, these challenging issues which are a significant area of research and study in DC-DC converters must be addressed in order to achieve better performance, which necessitates the use of a reliable closed-loop control system. From this perspective, traditional linear and nonlinear control methods have been proposed as good solutions. However, many studies from different fields [12, 16–18] have shown that nonlinear controllers outperform linear controllers in terms of disturbance rejection, small steady-state error, fast dynamic response, and low overshoot. Thus, the use of nonlinear control methods in a wide range of applications is rapidly broadening and growing at an unprecedented rate. The widespread use of various nonlinear control types for improving the behavior of buck converters can be found in the following studies: neuro-adaptive backstepping, [19] fuzzy logic, [20] sliding mode control, [10, 21–25] predictive control, [26] hierarchical control, [27] artificial neural network [28]. Among these control algorithms, the sliding mode control (SMC) has attracted a lot of interest because of its exceptional robustness against uncertainties and disturbances, simplicity in computational and implementation, fast dynamic response, guaranteed stability for all the operating conditions, and acceptable transient performance with respect to other controllers [21, 22, 29].

Since SMC improves the dynamic and static performances of systems such as buck converters and other power electronics circuits, it has been successfully applied to a wide range of linear and nonlinear systems besides power electronics, including bioreactor system, [17] robot manipulators, [29] coupled tank system, [18] and pendulum system [29]. However, it should be noted that SMC behaves differently in the field of power electronics because an ideal SMC means that the system should be operated at the highest possible switching frequency, which is unattainable in power electronics practical applications [4]. One of the proposed methods to make SMC applicable in power electronics circuits is hysteresis modulation (HM). This technique, which is essentially based on a special switching law bounded by two conditions, has been effectively implemented to power electronics circuits, particularly DC-DC converters [10, 16, 21, 23, 25] numerous times due to offering straightforward and simple implementation, not requiring additional computation or auxiliary circuitries [4]. Aside from these benefits, the most significant advantage it provides is that it translates an uncontrollable infinite switching frequency, which is undesirable in practice, into a limited and controllable switching frequency. In this way, unwanted high-frequency noises can be prevented. On the other hand, despite being a popular research subject, HM-based SMC brings with it the variable switching frequency problem. High and variable switching frequency causes excessive power losses, electromagnetic-interference (EMI) generation, and deteriorates the regulation properties of the converters [4, 22]. Hence, it is necessary to fix the switching frequency or at least limit its variation. For this purpose, SMC can be used to greatly enhance the switching frequency regulation of power converters as in output voltage regulation. At this point, SMC demonstrates its robustness as a controller once more. In contrast to the other controllers, it can simplify the solution to the aforesaid problem by utilizing its own internal structure (the assumption of piecewise linear behavior of the sliding function).

In recent years, SMC is preferred for controlling buck converters in many papers. In the majority of the papers, the conventional SMC (CSMC) method which employs a linear sliding surface based on the linear combination of the system states with a time-invariant coefficient [21] has been utilized. In order to obtain the fast dynamic response, large values are used as a coefficient. On the other hand, due to the asymptotic convergence property of the sliding surface, the state error signal cannot converge to zero in a finite time. Therefore, a relatively slow dynamic response and poor steady-state tracking problem may occur [30]. To address these issues and revamp the system's overall performance, terminal sliding mode control (TSMC) has been proposed. With respect to the CSMC, TSMC has a fractional power term in the sliding surface and uses a nonlinear sliding surface as well as offering some superior properties such as fast, finite-time convergence, better tracking precision [30, 31]. On the other hand, despite the advantages of TSMC, satisfactory time for convergence cannot be obtained when system states are away far from the equilibrium point [31]. This fact has stimulated researchers to dedicate a considerable effort to further enhanced control. Consequently, fast terminal sliding mode control (FTSMC) has been found for the above problem. This method combines the advantage of TMSC and CSMC [16, 31] and, hence, shows excellent transient response and convergence characteristics for both near and far away states from the equilibrium point [32]. FTSMC gets attention owing to its ability to attain a good dynamic performance and gradually is becoming the choice of many researchers for practical application.

In this paper, a modified FTSMC strategy is proposed for DC-DC buck converters. The main objective of the proposed method is to take the advantage of TMSC and CSMC simultaneously and then generate a regulated output voltage under the variations in the input voltage and load resistance. It is critical to fix the switching frequency in power electronics because high and variable switching frequency causes some undesirable outcomes. Therefore, another control

algorithm also has been presented to achieve fixed switching frequency. Furthermore, experimental results are obtained by using the voltage regulation controller in two separate scenarios under the same conditions: with and without switching frequency control strategy. In doing so, it is aimed to demonstrate the difference easily.

The rest of this paper is organized as follows: First, in Section 2, an analysis of the proposed converter is presented in order to facilitate the design of CSMC, TSMC, and FTSMC. Thereafter, CSMC, TSMC, and FTSMC are analyzed and compared with each other in Section 3. The theoretical considerations are verified by experimental studies, and obtained results are presented in Section 4. The determination of the parameters of the proposed control methods is also covered in this section. Finally, the conclusions are drawn in Section 5.

## 2. Modeling of the DC-DC Buck Power Converter

The circuit model of the buck converter is depicted in Figure 1. Clearly, it consists of an inductor, a capacitor ($C$), a semiconductor switch $S_w$, and a diode ($D$). Input voltage, load resistance, and output current are denoted with $E$, $R$, and $I_0$, respectively. During the modeling of power converters, the converter parameters and power switch were assumed to be ideal [1].

The state equations describing the operation of the proposed converter can be written for the switching conditions ON and OFF as (1) and (2), respectively [21]. It is worth noting that the parasitic parameters are neglected for simplicity.

$$\begin{bmatrix} \dot{I}_L \\ \dot{V}_0 \end{bmatrix} = \begin{bmatrix} 0 & \frac{-1}{L} \\ \frac{1}{C} & \frac{-1}{RC} \end{bmatrix} \begin{bmatrix} I_L \\ V_0 \end{bmatrix} + \begin{bmatrix} \frac{1}{L} \\ 0 \end{bmatrix} E, \tag{1}$$

and

$$\begin{bmatrix} \dot{I}_L \\ \dot{V}_0 \end{bmatrix} = \begin{bmatrix} 0 & \frac{-1}{L} \\ \frac{1}{C} & \frac{-1}{RC} \end{bmatrix} \begin{bmatrix} I_L \\ V_0 \end{bmatrix} + \begin{bmatrix} 0 \\ 0 \end{bmatrix} E, \tag{2}$$

where $I_L$ is the inductor current and $V_0$ is the output voltage. Combining (1) and (2) gives the average state space model of the buck converter as in the following matrix:

$$\begin{bmatrix} \dot{I}_L \\ \dot{V}_0 \end{bmatrix} = \begin{bmatrix} 0 & \frac{-1}{L} \\ \frac{1}{C} & \frac{-1}{RC} \end{bmatrix} \begin{bmatrix} I_L \\ V_0 \end{bmatrix} + \begin{bmatrix} \frac{u}{L} \\ 0 \end{bmatrix} E, \tag{3}$$

where $u$ is the control input which takes "0" for the OFF state and "1" for the ON state of the switch. For simplicity of mathematical expressions as well as making the proposed controller design easier, new definitions based on output voltage error are defined in the following equations:

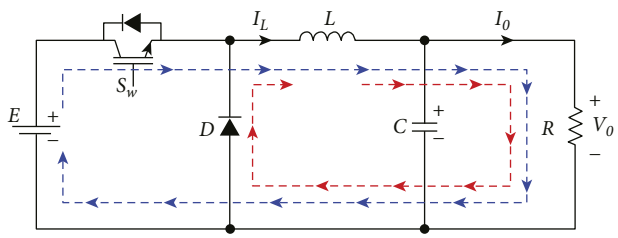


Figure 1: The circuit model of the buck converter (blue line: the switch is on; red line: the switch is off).

$$x_1 = V_0 - V_{\text{ref}}, \tag{4}$$

$$x_2 = \dot{x}_1 = \dot{V}_0 - \dot{V}_{\text{ref}} = \dot{V}_0, \tag{5}$$

where $\dot{x}_1$ denotes the derivative of $x_1$, and $V_{\text{ref}}$ is the reference voltage for the output terminal. By taking the time derivative of (4), the voltage error $x_1$ and its derivative $x_2$ dynamics can be obtained as (6) and (7), respectively.

$$\dot{x}_1 = x_2, \tag{6}$$

$$\dot{x}_2 = -\frac{x_2}{RC} + \frac{1}{LC}\left(uE - V_{\text{ref}} - x_1\right). \tag{7}$$

## 3. Control Methods

*3.1. Conventional Sliding Mode Control.* The fundamental design of SMC is accomplished through two necessary requirements. One of the two requirements is an appropriate sliding manifold [22]. Hence, for the CSMC design based on (4) and (5), the sliding surface $S$ can be written as in the following equation [21]:

$$S_{\text{CSMC}} = \lambda x_1 + x_2, \quad \lambda > 0, \tag{8}$$

where $\lambda$ is always a positive constant for achieving system stability. The solution of (8) in steady-state is expressed as (9) [33] by imposing $S_{\text{CSMC}} = 0$ in (8).

$$x_1(t) = x_1(t_0)e^{-\lambda t}. \tag{9}$$

Since $x_1$ symbolizes the error, the linear sliding surface can guarantee the asymptotic error convergence in the sliding mode, which means the output error will not converge to zero in finite time [32, 33]. In order to obtain a fast transient response, i.e., decreasing the time of convergence, the large value of $\lambda$ can be preferred as shown in Figure 2. On the other hand, the system errors still cannot converge to zero in finite time [21]. To address this issue, i.e., to enhance the asymptotic convergence to a finite time state convergence, [34] a new SMC scheme known as TSMC has been suggested.

*3.2. Terminal Sliding Mode Control.* The sliding surface for the TSMC is defined by the following equation [35]:

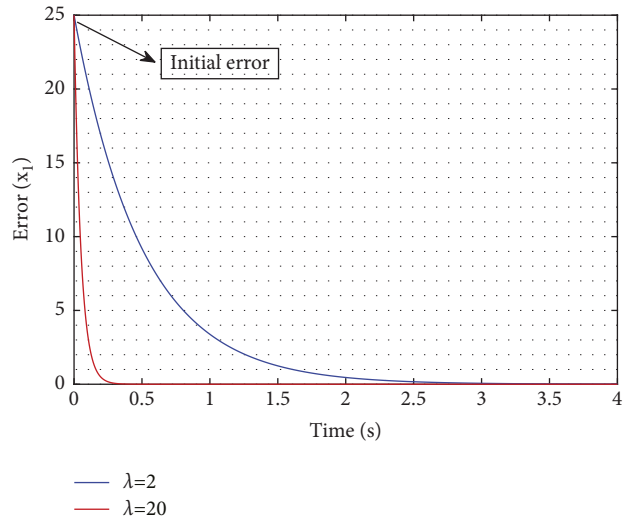


Figure 2: Error trajectory of CSMC with different values of $\lambda$.

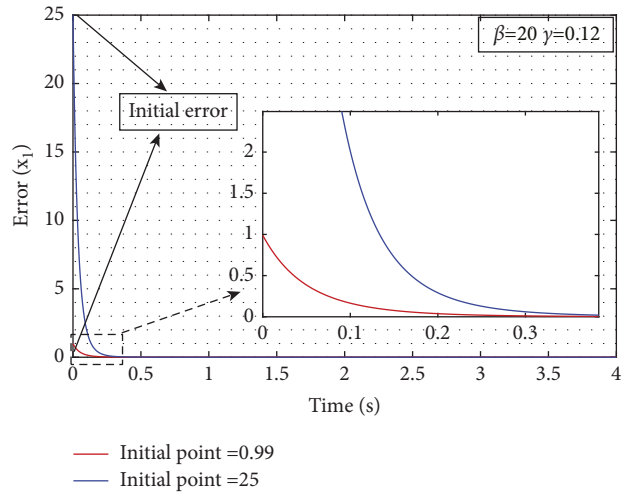


Figure 3: Error trajectory of TSMC with different initial values.

$$S_{\mathrm{TSMC}} = \dot{x}_1 + \beta x_1^{(q/p)}, \tag{10}$$

where $\beta > 0$ is a constant, and $0 < (\gamma = q/p) < 1$ where $p$ and $q$ are positive odd integers, which satisfy the condition $p > q$. By employing the nonlinear term $x_1^{q/p}$ into the sliding surface, the TSMC has a better performance to speed up the rate of convergence towards equilibrium in finite time [23, 31, 32]. The time can be found as (11) [33] by solving the differential equation (10).

$$t^{\mathrm{TSMC}} = \frac{p}{\beta(p-q)} \left| x_1(t_0) \right|^{(1-(q/p))}. \tag{11}$$

To see the finite time convergence of TMSC, (11) can be investigated. Equation (11) clearly shows that equation (10) can provide a finite-time convergence of the error from a starting point to an equilibrium position [21, 33] which is unattainable for CSMC. Notice that $t^{\mathrm{TSMC}}$ depends on parameters $(\beta, \gamma)$ and initial point as can be seen from (11). On the other hand, TSMC has some flaws that make it difficult to achieve satisfactory results. Firstly, with Figure 3, the performance of convergence is deteriorated when initial error is far away ($|x_1| > 0$, blue line) from equilibrium point [32, 36]. Secondly, as shown in Figure 4(a), comparison with CSMC, TSMC provides an acceptable convergence time when initial error is far away from equilibrium, but it presents poor convergence performance and long convergence time when compared to the CSMC if the initial error is near equilibrium as demonstrated in Figure 4(b). The explanation of this predicament is that when the initial error is far away from the equilibrium point, the term $x_1^{q/p}$ tends to increase the magnitude of the convergence rate, i.e., the dynamical system converges rapidly. To overcome this challenge, a popular approach which is known as FTSMC has been presented.

*3.3. Fast Terminal Sliding Mode Control.* Sliding surface for the FTSMC can be written as in the following equation [37]:

$$S_{\mathrm{FTSMC}} = \dot{x}_1 + \lambda x_1 + \beta x_1^{q/p}. \tag{12}$$

Comparing with the TSMC, an additional linear term has been defined in the FTSMC's sliding surface. By introducing a linear term in (12), system states reach at the equilibrium point in a shorter time [37]. The convergence time can be expressed as (13) [33]. Equation (13) expresses the exact convergence time to equilibrium point from an initial point for FTSMC. Similar to $t^{\mathrm{TSMC}}$ in (11), $t^{\mathrm{FTSMC}}$ also depends on parameters $(\beta, \gamma)$ and initial state.

$$t^{\mathrm{FTSMC}} = \frac{p}{\beta(p-q)} \left( \ln\left( \lambda x_1(t_0)^{1-(q/p)} + \beta \right) - \ln \beta \right). \tag{13}$$

As demonstrated in Figure 5, different from TMSC, FTSMC exhibits unique convergence characteristics when initial values are either far away ($|x_1| > 0$) from or near ($|x_1| < 0$) equilibrium. In addition, the convergence performance of FTSMC at far away initial values ($|x_1| > 0$, red line) is even superior to the performance of TSMC at near initial values ($|x_1| < 0$, black line).

With the help of the recommended FTSMC strategy, the performance of the closed-loop system can be improved compared to ordinary TSMC and CSMC. As it can be seen from (8) and (10), FTSMC is a hybrid combination of TSMC and CSMC [16]. Hence, the suggested approach is well-performed than TSMC and CSMC in terms of driving error remission capability within finite time, fast convergence tract, lower steady-state error, providing a high convergence rate even when the states are at a distance from the equilibrium point [31, 32, 36, 37].

As detaily studied in Reference 37, the fast convergence property of (12) can be explained using the structure of the fast terminal sliding surface. When the system reaches and moves on the sliding surface, i.e., $S_{\mathrm{FTSMC}} = 0$, then the equation of (12) can be described as shown in the following equation:

$$\dot{x}_1 = -\underbrace{\lambda x_1}_{\text{first term}} - \underbrace{\beta x_1^{(q/p)}}_{\text{second term}}. \tag{14}$$

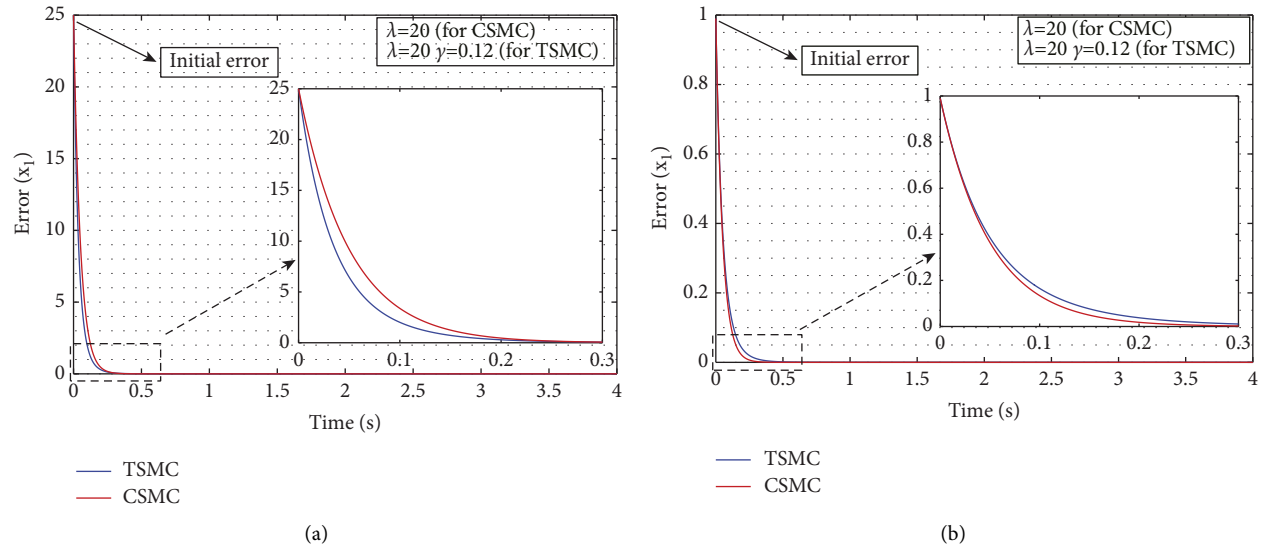


Figure 4: Error trajectory of TSMC and CSMC: (a) far away initial value; (b) near initial value.

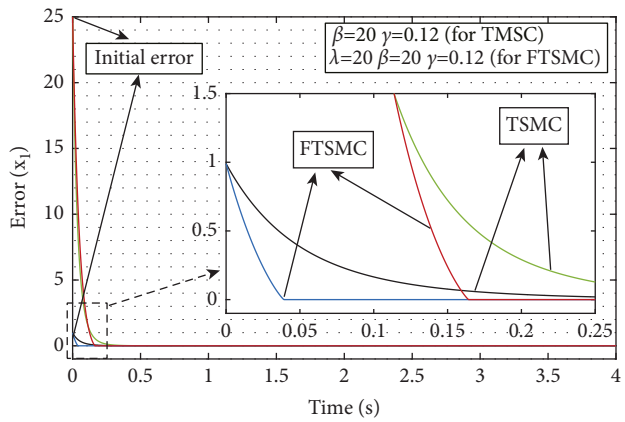


Figure 5: Comparison of error trajectory of FTSMC and TSMC for far away and near initial values.

When $x_1$ is far away from equilibrium point, the first term of (14) has an important effect on dynamics whereas the second term of (14) plays a small role. Therefore, the first term of (14) dominates over the second term of (14). In this case, (12) becomes approximately as $\dot{x}_1 = -\lambda x_1$. When $x_1$ is close to equilibrium point, the second term of (14) plays a crucial role whereas the first term of (14) has a small effect on dynamics. Hence, the second term of (14) has the upper hand to the first term of (14). In this case, (12) becomes approximately as $\dot{x}_1 = -\beta x_1^{(q/p)}$.

*3.4. Selection Surface for Fast Terminal Sliding Mode Control.* Inspired by the study in Reference 35, a modified fast terminal sliding surface is used in this paper instead of (12). Modification was made by taking the absolute value of the nonlinear term of the surface in equation (12) and multiplying the same expression with the sign function. By doing so, a more robust surface function is obtained. For $x_1 < 0$, the fractional power $(q/p)$ may cause $x_1^{q/p} \notin R$ in (12). In this case, $S_{\text{FTSMC}} \notin R$. For the surface in (12), unfavorable outcomes may be obtained in the case of $x_1 < 0$. To cope with the mentioned problem, the sliding surface in (15) which is slightly different from the previously given in (12) is presented. $S_{FTSMC} \in R$ is guaranteed by using (15) [16].

Sliding surface for the modified FTSMC is introduced as follows:

$$S_{\text{FTSMC}} = \dot{x}_1 + \lambda x_1 + \beta |x_1|^{\gamma} \text{sign}(x_1). \tag{15}$$

To see the convergence performance of the modified method, Figure 6 has been drawn. It is obvious from Figure 6(a), for the case of near initial values, the suggested technique has a shorter convergence time than CSMC, whereas TMSC lags behind CSMC. Furthermore, the proposed strategy also presents an excellent convergence performance in the case of faraway initial values when compared to CSMC and TSMC as shown in Figure 6(b). It is worth noting that the parameters given in the boxes were used to generate convergence graphs.

*3.5. Switching Control Strategy.* Another requirement for designing SMC is a suitable control law [22]. A common switching control law can be given as follows [21]:

$$u = \frac{1}{2}\left(1 - \text{sign}\left(S_{\text{FTSMC}}\right)\right) = \begin{cases} 1, & \text{when } S_{\text{FTSMC}} < 0, \\ 0, & \text{when } S_{\text{FTSMC}} > 0. \end{cases} \tag{16}$$

A switching function must be employed so that the system's state trajectory at any initial location hits the sliding surface. This is referred to as the hitting condition, which is satisfied by the control law in (16), and it is one of the three prerequisites for SM control operation to occur [22]. From (16), the state trajectory of the system, in which every point above the sliding line $(S_{\text{FTSMC}} > 0)$ can only converge towards the sliding surface when the switching function becomes $u = 0$. In this case, the switch $S_w$ is OFF. Conversely, the system's state trajectory, where

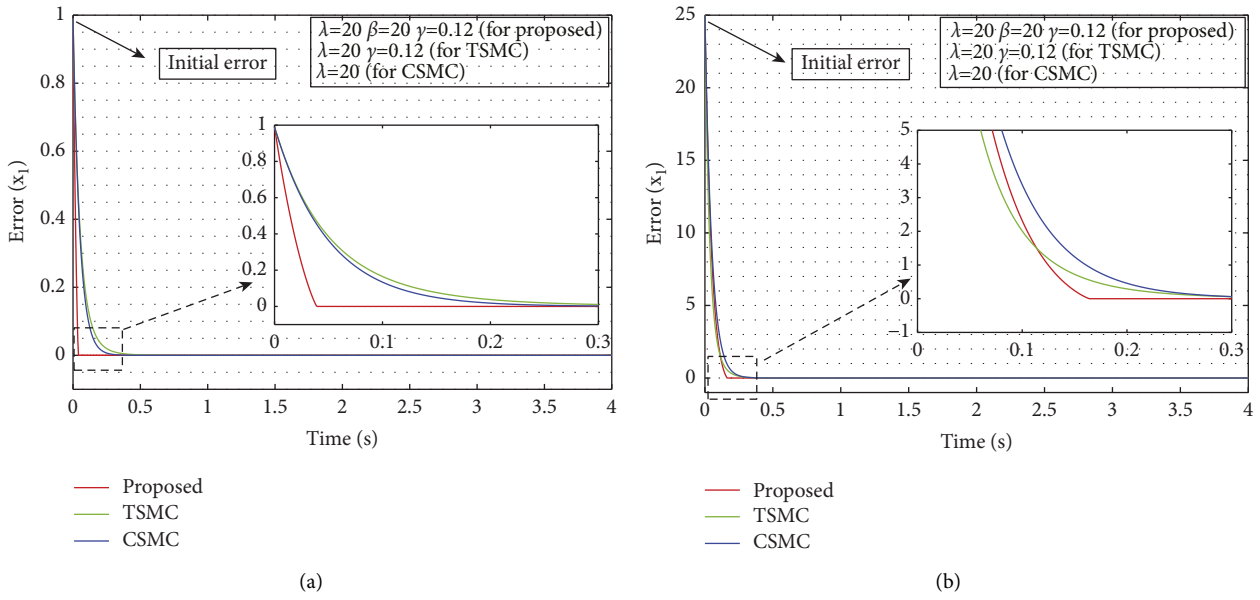


Figure 6: Error trajectory of TSMC, CSMC, and proposed method: (a) near initial error; (b) far away initial error.

any arbitrary location below the sliding line ($S_{\text{FTSMC}} < 0$) will strike the sliding surface only when the switching function becomes $u = 1$. In this case, the switch $S_w$ is ON [4, 22].

As it can be realized from (16), the control law has a signum function sign $(\cdot)$. However, this discontinuous function leads to unlimited and uncontrollable switching frequency, i.e., causes chattering in the control signal [23, 38]. The chattering is harmful because, in practical applications, it results in poor control accuracy, [39] excessive wear of moving mechanical parts, and high heat losses in power circuits [29]. Furthermore, a practical system cannot switch at infinite frequency [4]. To make the control law applicable while alleviating the effect of the aforementioned problems, the hysteresis modulation (HM) method which is commonly used as a classical solution in literature is presented in this paper. The method is defined in the following equation:

$$u = \begin{cases} 1, & \text{when } S_{\text{FTSMC}} < -\Delta, \\ 0, & \text{when } S_{\text{FTSMC}} > \Delta, \\ \text{keep previous position}, & \text{when otherwise}, \end{cases} \quad (17)$$

where $\Delta$ is a hysteresis bandwidth that can be set to any suitable value. The goal of using a constant bandwidth with the boundary conditions $S_{\text{FTSMC}} = \Delta$ and $S_{\text{FTSMC}} = -\Delta$ is to provide a control law to limit the converter's switching frequency ($f_s$) [22, 40]. Note that (17) simply expresses that the switch of the proposed converter will turn off when $S_{\text{FTSMC}} > \Delta$. Similarly, when $S_{\text{FTSMC}} < -\Delta$, the switch of the buck converter will turn on. If $-\Delta \le S_{\text{FTSMC}} \le \Delta$, the switch of the converter will keep the previous position. In the region $-\Delta \le S_{\text{FTSMC}} \le \Delta$, no switching takes place, and thus, unlimited and uncontrollable switching frequency of the sliding mode can be restricted and controlled [22].

Figure 7 simply confirms that when the switch is ON, i.e., in $T_{\text{on}}$, function $S_{\text{FTSMC}}$ must increase, while when it is OFF, i.e., in $T_{\text{off}}$, function $S_{\text{FTSMC}}$ must decrease [41]. Switching

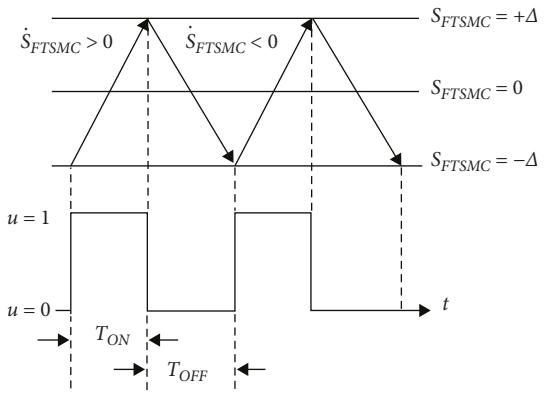


Figure 7: Hysteresis modulated sliding function.

frequency of the converter can be obtained by using the derivatives of $S_{\text{FTSMC}}$, with the help of Figure 7. In order to find the frequency, $\dot{S}_{\text{FTSMC}}$ is obtained as follows [16]:

$$\begin{aligned} \dot{S}_{\text{FTSMC}} &= x_1 + \lambda \dot{x}_1 + \beta\gamma |x_1|^{\gamma-1} \dot{x}_1, \\ &= \dot{x}_2 + \left(\lambda + \beta\gamma |x_1|^{\gamma-1}\right) x_2, \\ &= -\frac{x_2}{RC} + \frac{1}{LC}\left(uE - V_{ref} - x_1\right) + \left(\lambda + \beta\gamma |x_1|^{\gamma-1}\right) x_2. \end{aligned} \quad (18)$$

$(\dot{S}_{\text{FTSMC}})^+$ and $(\dot{S}_{\text{FTSMC}})^-$ are considered as the positive slope and negative slope of the time derivatives of sliding surface $S_{\text{FTSMC}}$, i.e., $\dot{S}_{\text{FTSMC}} > 0$ and $\dot{S}_{\text{FTSMC}} < 0$, for ON and OFF states of the switch $S_w$, respectively.

For ON state: if $S_{\text{FTSMC}} < 0$, then $\dot{S}_{\text{FTSMC}} > 0$, so $u = 1$, then a positive slope can be obtained as follows:

$$\begin{aligned} \left(\dot{S}_{FTSMC}\right)^+ &= -\frac{x_2}{RC} + \frac{1}{LC}\left(E - V_{ref} - x_1\right) \\ &\quad + \left(\lambda + \beta\gamma |x_1|^{\gamma-1}\right) x_2. \end{aligned} \quad (19)$$

For OFF state: if $S_{\mathrm{FTSMC}} > 0$, then $\dot{S}_{\mathrm{FTSMC}} < 0$, so $u = 0$, and then, negative slope can be obtained as follows:

$$\left(\dot{S}_{\mathrm{FTSMC}}\right)^{-} = -\frac{x_2}{RC} + \frac{1}{LC}\left(-V_{ref} - x_1\right) + \left(\lambda + \beta\gamma\left|x_1\right|^{\gamma-1}\right)x_2. \quad (20)$$

With the help of (19) and (20), ON and OFF states of the switch $S_w$ are written as follows:

$$T_{\mathrm{on}} = \frac{2\Delta}{\left(\dot{S}_{\mathrm{FTSMC}}\right)^{+}} = \frac{2\Delta}{-\left(x_2/\mathrm{RC}\right) + \left(1/\mathrm{LC}\right)\left(E - V_{\mathrm{ref}} - x_1\right) + \left(\lambda + \beta\gamma\left|x_1\right|^{\gamma-1}\right)x_2}, \quad (21)$$

$$T_{\mathrm{off}} = \frac{-2\Delta}{\left(\dot{S}_{\mathrm{FTSMC}}\right)^{-}} = \frac{-2\Delta}{-\left(x_2/\mathrm{RC}\right) + \left(1/\mathrm{LC}\right)\left(-V_{\mathrm{ref}} - x_1\right) + \left(\lambda + \beta\gamma\left|x_1\right|^{\gamma-1}\right)x_2}. \quad (22)$$

Hence, the switching frequency can be calculated as follows:

$$\begin{aligned} f_s &= \frac{1}{T_{\mathrm{on}} + T_{\mathrm{off}}} = \left(\frac{2\Delta}{\left(\dot{S}_{\mathrm{FTSMC}}\right)^{+}} - \frac{2\Delta}{\left(\dot{S}_{\mathrm{FTSMC}}\right)^{-}}\right)^{-1} \\ &= \left(\frac{2\Delta}{-\left(x_2/\mathrm{RC}\right) + \left(E - V_{\mathrm{ref}} - x_1/\mathrm{LC}\right) + \left(\lambda + \beta\gamma\left|x_1\right|^{\gamma-1} - \left(1/\mathrm{RC}\right)\right)x_2} - \frac{2\Delta}{-\left(x_2/\mathrm{RC}\right) + \left(-V_{\mathrm{ref}} - x_1/\mathrm{LC}\right) + \left(\lambda + \beta\gamma\left|x_1\right|^{\gamma-1} - \left(1/\mathrm{RC}\right)\right)x_2}\right)^{-1}. \end{aligned} \quad (23)$$

Assume those error variables $(x_1, x_2)$ are negligible in the steady-state, [21] then (23) can be simplified as follows:

$$f_s = \frac{V_{\mathrm{ref}}}{2\Delta\mathrm{LC}}\left(1 - \frac{V_{\mathrm{ref}}}{E}\right). \quad (24)$$

As can be seen from (24), the switching frequency is inversely proportional to the hysteresis bandwidth Δ. By choosing an appropriate hysteresis bandwidth, a suitable switching frequency can be obtained. However, this control strategy suffers from a variable switching frequency. Because, as can be seen from 24, the switching frequency increases as the input voltage increases and drops as the input voltage falls. Similarly, with an increase in the reference value of the output voltage, the switching frequency lowers, and with a decrease in the reference value of the output voltage, the switching frequency increases. These variations in switching frequency result in switching and gate-driven power losses, which downgrade the accuracy and reliability of the whole system, especially, in terms of power conversion efficiency. Besides, the lost energy generates heat, which, if not effectively dispersed, might shorten the system's lifespan. Therefore, to avoid operating the converter at a different switching frequency than the one designed for it, several innovative researches has been offered to either fix or limit the variations of switching frequency [38, 42–45]. Among these studies, Reference 38 describes a simple hysteresis band controller which regulates the switching frequency to a predefined desired constant value without the use of additional control components, a perfect knowledge of all the states in the system (hence, no need for many sensors), or complicated calculations (in the duty cycle computation).

In Reference 38, a control technique based on a hysteresis band comparator was developed to regulate the switching frequency. The technique adds a new loop that measures the switching period, uses a frequency controller loop (FCL) to update the hysteresis band value, and enforces the measured switching period $(T_s)$ to converge to a preassigned reference (Ts_ref). The FCL in Reference 38 is a discrete-time integrator, and the implementation of the control is required using a digital control platform. The study also includes the FCL's comprehensive design approach as well as the switching frequency control system's stability analysis. In order to get a fixed switching-frequency operation, this work uses the FCL scheme. By following the steps given in Reference 38, the design of the FLC for this study is given in the experimental results section.

*3.6. Existence of Fast Terminal Sliding Mode Control.* Another prerequisite for SMC operation to occur is the existence condition [22]. The condition for checking the existence of a sliding mode control, Lyapunov's second theory is used as a sufficient method. The aim of using this method is to ensure that the movement of the error variables stays on the sliding surface [23]. To check the existence of modified FTSMC, firstly, a positive definite Lyapunov function candidate is selected as $V = (1/2)(S_{\mathrm{FTSMC}})^2$. The time derivative of the Lyapunov function candidate must be negative in order to check the existence condition [29].

$$\lim_{S_{\mathrm{FTSMC}} \longrightarrow 0}\left(S_{\mathrm{FTSMC}}\dot{S}_{\mathrm{FTSMC}}\right) < 0, \tag{25}$$

$$\lim_{S_{\mathrm{FTSMC}} \longrightarrow 0^{-}}\left(\dot{S}_{\mathrm{FTSMC}}\right) > 0, \tag{26}$$

$$\lim_{S_{\mathrm{FTSMC}} \longrightarrow 0^{+}}\left(\dot{S}_{\mathrm{FTSMC}}\right) < 0. \tag{27}$$

Mathematically to satisfy (25), two constraints are given as follows:

Case 1: Based on equation (26), if $S_{\mathrm{FTSMC}} < 0$, then $\dot{S}_{\mathrm{FTSMC}}$ must be positive. In this case, the control law $u$ takes the value $1\,(u = 1)$ as seen in Figure 7. By using (18) and considering $u = 1$, the following inequality can be written as follows:

$$\% -\frac{x_2}{RC} + \frac{1}{LC}\left(E - V_{ref} - x_1\right) + \left(\lambda + \beta\gamma\left|x_1\right|^{\gamma-1}\right)x_2 > 0. \tag{28}$$

Case 2: Based on (27), when $S_{\mathrm{FTSMC}} > 0$, then $\dot{S}_{\mathrm{FTSMC}}$ needs to be negative. In this case, the control law $u$ will turn the value $0\,(u = 0)$ as seen in Figure 7. Considering (18) and $u = 0$, the following inequality is derived:

$$-\frac{x_2}{RC} + \frac{1}{LC}\left(-V_{\mathrm{ref}} - x_1\right) + \left(\lambda + \beta\gamma\left|x_1\right|^{\gamma-1}\right)x_2 < 0. \tag{29}$$

The above equations, i.e., (28) and (29), show the sliding mode dynamics for the closed loop [21] modified FTSMC system. When the inequalities in (28) and (29) are held, the existence condition can be guaranteed and a stable system is obtained. (28) and (29) are combined in a new inequality as follows:

$$\frac{-E_{\min}}{\mathrm{LC}} < \frac{1}{\mathrm{LC}}\left(-V_{\mathrm{ref}} - x_1\right) + \left(\lambda + \beta\gamma\left|x_1\right|^{\gamma-1} - \frac{1}{R_{(\min)}C}\right)x_2 < 0. \tag{30}$$

Based on (30), the parameters $\beta$, $\lambda$, and $\gamma$ in (15) can be determined. However, it should be noted that it is difficult to find the values of control parameters by using (30). To make the process of selecting parameters that satisfy the existence condition more straightforward, (4) and (5) are substituted into (30) as shown in (31). It can be seen that the inequality includes $I_L$ and $V_0$ which are instantaneous state variables. The consideration of the time-varying nature of these components undesirably complicates the design. In this paper, a static sliding surface is used. When designing a sliding mode controller with a static surface, ensuring the existence condition for the steady-state operation can be specified as a practical approach. With these considerations, the state variables $I_L$ and $V_0$ can be replaced with their steady-state values. This ensures that the existing condition is satisfied at least in the vicinity of the equilibrium point, [4] as well as providing a convenient way to identify control parameters. Therefore, (30) can be rewritten as follows:

$$\frac{-E_{(\min)}}{\mathrm{LC}} < -\frac{1}{\mathrm{LC}}\left(V_{0(\mathrm{SS})}\right) + \left(\lambda + \beta\gamma\left|V_{0(\mathrm{SS})} - V_{\mathrm{ref}}\right|^{\gamma-1} - \frac{1}{R_{(\min)}C}\right)\left(\frac{I_{L_{(\mathrm{SS})}}}{C} - \frac{V_{0(\mathrm{SS})}}{R_{(\min)}C}\right) < 0. \tag{31}$$

*3.7. Stability Analysis of Fast Terminal Sliding Mode Control.* The final prerequisite for SMC operation is stability analysis [22]. The stability of the system can be proved by Lyapunov's stability theory. In order to achieve this, the Lyapunov function is considered as $V = (1/2)(S_{\mathrm{FTSMC}})^2$. Its time derivative is obtained as follows:

$$\begin{aligned}\dot{V} &= S_{\mathrm{FTSMC}}\dot{S}_{\mathrm{FTSMC}},\\ &= S_{\mathrm{FTSMC}}\left[\frac{1}{\mathrm{LC}}\left(uE - V_{\mathrm{ref}} - x_1\right) + \left(\lambda + \beta\gamma\left|x_1\right|^{\gamma-1} - \frac{1}{\mathrm{RC}}\right)x_2\right].\end{aligned} \tag{32}$$

Considering Case 1, (32) can be written as follows:

$$\dot{V} = S_{\mathrm{FTSMC}}\left[\frac{1}{\mathrm{LC}}\left(E - V_{\mathrm{ref}} - x_1\right) + \left(\lambda + \beta\gamma\left|x_1\right|^{\gamma-1} - \frac{1}{\mathrm{RC}}\right)x_2\right]. \tag{33}$$

Similarly, based on Case 2, (32) can be obtained as follows:

$$\dot{V} = S_{\mathrm{FTSMC}}\left[\frac{1}{\mathrm{LC}}\left(-V_{\mathrm{ref}} - x_1\right) + \left(\lambda + \beta\gamma\left|x_1\right|^{\gamma-1} - \frac{1}{\mathrm{RC}}\right)x_2\right]. \tag{34}$$

The combination of (32), (33), and (34) gives (35).

$$\begin{aligned}\dot{V} &= S_{\mathrm{FTSMC}}\left[\frac{E}{2\mathrm{LC}} - \frac{V_{\mathrm{ref}} + x_1}{\mathrm{LC}} + \left(\lambda + \beta\gamma\left|x_1\right|^{\gamma-1} - \frac{1}{\mathrm{RC}}\right)x_2\right] - \left|S_{\mathrm{FTSMC}}\right|\frac{E}{2\mathrm{LC}},\\ &= \left|S_{\mathrm{FTSMC}}\right|\mathrm{sign}\left(S_{\mathrm{FTSMC}}\right)\left[\frac{E}{2\mathrm{LC}} - \frac{V_{\mathrm{ref}} + x_1}{\mathrm{LC}} + \left(\lambda + \beta\gamma\left|x_1\right|^{\gamma-1} - \frac{1}{\mathrm{RC}}\right)x_2\right] - \left|S_{\mathrm{FTSMC}}\right|\frac{E}{2\mathrm{LC}},\\ &= \left|S_{\mathrm{FTSMC}}\right|\left(\mathrm{sign}\left(S_{\mathrm{FTSMC}}\right)\left[\frac{E}{2\mathrm{LC}} - \frac{V_{\mathrm{ref}} + x_1}{\mathrm{LC}} + \left(\lambda + \beta\gamma\left|x_1\right|^{\gamma-1} - \frac{1}{\mathrm{RC}}\right)x_2\right] - \frac{E}{2\mathrm{LC}}\right).\end{aligned} \tag{35}$$

The following inequality can be obtained by using the following equation:

$$\dot{V} \le |S_{\text{FTSMC}}|\left(\left|\frac{E}{2\text{LC}} - \frac{V_{\text{ref}} + x_1}{\text{LC}} + \left(\lambda + \beta\gamma|x_1|^{\gamma-1} - \frac{1}{\text{RC}}\right)x_2\right| - \frac{E}{2\text{LC}}\right). \tag{36}$$

The derivative of the Lyapunov function must be negative definite ($\dot{V} < 0$) so as to satisfy the stability of the system [4]. It would be guaranteed that $\dot{V} < 0$ if the following inequality is satisfied.

$$\left|\frac{E}{2\text{LC}} - \frac{V_{\text{ref}} + x_1}{\text{LC}} + \left(\lambda + \beta\gamma|x_1|^{\gamma-1} - \frac{1}{\text{RC}}\right)x_2\right| - \frac{E}{2\text{LC}} < 0. \tag{37}$$

As long as appropriate values for parameters $\lambda$, $\beta$ and $\gamma$ are chosen, stability of modified FTSMC can be obtained. From (28), (29), and (37), it can be concluded that the parameter selection is critical in order to satisfy both the existence and stability conditions. The values of the coefficients we use in the experimental application are as follows: $\lambda = 3600$, $\beta = 10$, $\gamma = 0.2$. The requirement mentioned in (37) is satisfied in a steady state, as shown in Figure 8 which is produced with above coefficients and nominal values of the converter parameters. Satisfying (37) demonstrates the effectiveness of the proposed surface, because it is much more difficult to meet (37) for some other FTSM surfaces.

*3.8. Equivalent Control.* It is important to find an equivalent control in order to ensure that the error variables are maintained on the selected surface [21, 23]. The equivalent control, denoted by $u_{\text{eq}}$ is derived through the invariance condition given by the following equation [29]:

$$\frac{\text{d}\left(S_{\text{FTSMC}}\right)}{\text{d}t}_{\substack{S_{\text{FTSMC}}=0 \\ u=u_{\text{eq}}}} = 0. \tag{38}$$

Then, the equivalent control can be obtained as follows:

$$u_{\text{eq}} = \frac{\text{LC}}{E}\left[x_2\left(\frac{1}{\text{RC}} - \lambda - \beta\gamma|x_1|^{\gamma-1}\right) + \frac{V_{\text{ref}} + x_1}{\text{LC}}\right]. \tag{39}$$

As mentioned before, the equivalent control keeps dynamic variables on the selected surface. However, this control might not be enough to bring the system states to an equilibrium point from an initial point [16, 21]. Hence, an additional switching action is added to the equivalent control structure as shown in (39). Now, the final control input can be written as follows:

$$u = \frac{\text{LC}}{E}\left[x_2\left(\frac{1}{\text{RC}} - \lambda - \beta\gamma|x_1|^{\gamma-1}\right) + \frac{V_{\text{ref}} + x_1}{\text{LC}} - k\,\text{sign}\left(S_{\text{FTSMC}}\right)\right], \tag{40}$$

where $k$ is the switching control gain.

*3.9. Robustness Analysis.* Power electronic converters suffer disturbances and uncertainties. The controllers designed for power converters are expected to regulate the output voltage and current while also dealing with disturbances and uncertainties. Therefore, to investigate the robustness of the controllers against parametric uncertainties and external disturbances, equation (7) can be rewritten as follows:

$$\dot{x}_2 = -\frac{x_2}{\text{RC}} + \frac{1}{\text{LC}}\left(uE - V_{\text{ref}} - x_1\right) + d(t), \tag{41}$$

where $d(t)$ represent external disturbances and parametric uncertainties, i.e. the parameters of (3) are partially unknown. Then substituting (40) and (41) into (25) yields.

$$\begin{aligned} \dot{V} &= S_{\text{FTSMC}}\dot{S}_{\text{FTSMC}} < 0, \\ &= S_{\text{FTSMC}}\left(\dot{x}_2 + \left(\lambda + \beta\gamma|x_1|^{\gamma-1}\right)x_2\right) < 0, \\ &= S_{\text{FTSMC}}\left(d(t) - k\,\text{sign}\left(S_{\text{FTSMC}}\right)\right) < 0. \end{aligned} \tag{42}$$

It can be concluded from (42), and it is possible to eliminate the effect of external disturbances and parametric uncertainties as long as a suitable value for the switching control gain that satisfy $|d(t)| < k$ is chosen.

## 4. Implementation of Proposed Controllers and Experimental Results

To further assess the performance and effectiveness of the proposed approach, an experimental prototype for both output voltage regulation and switching frequency control of the buck converter has been constructed, and the findings of the experiment are presented in this section. The prototype consists of a buck converter, an adjustable DC power supply, resistive load, a voltage sensor, a microcontroller (TMS320F28379D) assisted Matlab/Simulink. The specifications of the buck converter are given in Table 1.

As shown in Figure 9, the backward Euler technique has been designed in Matlab/Simulink software for the experimental test to avoid utilizing a current sensor for the capacitor. By doing so, both the cost of the system is reduced, and the voltage distortion caused by the capacitor current sensor is prevented. In terms of computational burden, compared to the conventional FTSMC method, the proposed method needs one absolute and one sign function, additionally. Therefore, the execution times of both algorithms are very close to each other (conventional FTSMC: 17.4 $\mu$s and proposed method: 17.9 $\mu$s). Consequently, the increment in the computational power requirement is less. Since some delays may occur during the control operations, the sampling time is defined as 25 $\mu$s to prevent overtime error.

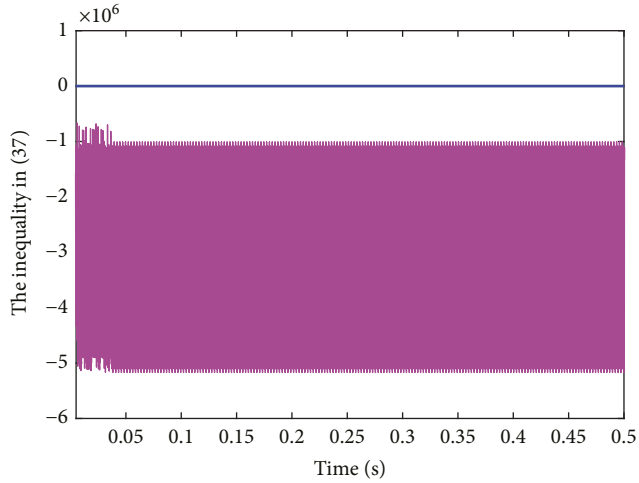


Figure 8: Steady-state for the inequality in (37) with the proposed surface.

Table 1: Buck converter parameters.

| Parameter | Value |
|---|---|
| Input voltage, $E$ | 15 V–25 V |
| Inductance, $L$ | 1 mH |
| Load resistance, $R$ | 10 Ω–5 Ω |
| Capacitance, $C$ | 1000 $\mu$F |
| Output voltage reference, $V_{ref}$ | 12 V–7 V |
| Switching period reference, Ts_ref | 5 kHz |

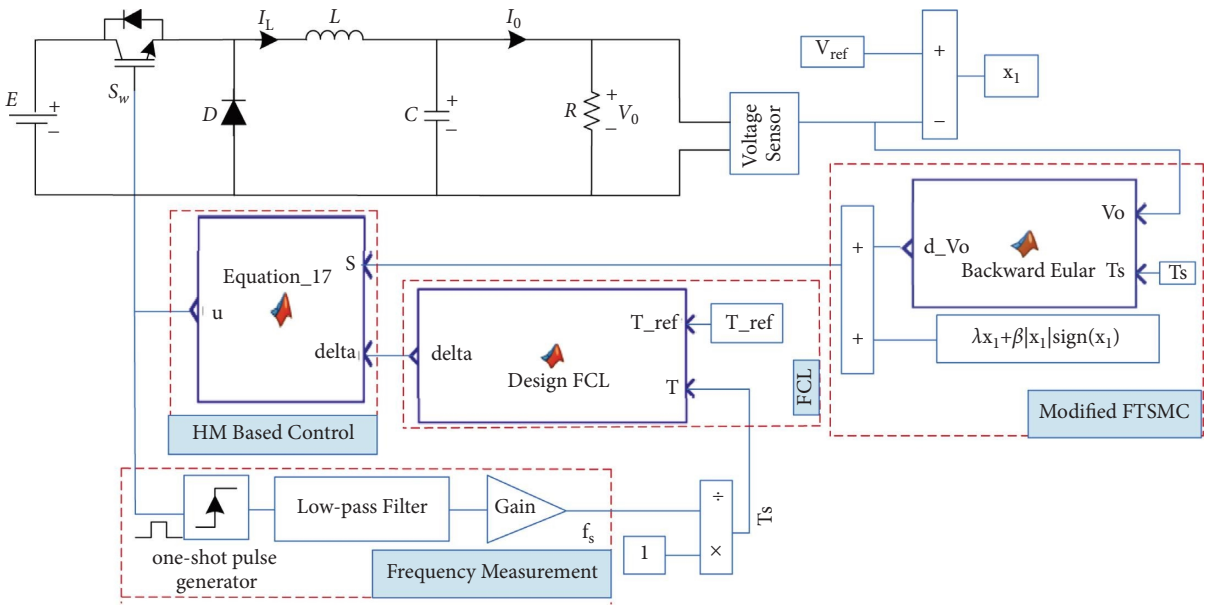


Figure 9: Block diagram of the buck converter with controllers.

*4.1. Determination of Modified FTSMC Coefficients.* As previously stated, the satisfaction of the conditions which are dependent on coefficients given in (31) and (37) is significant for the system. To make parameter selection easier while adhering to (31) and (37) inequalities, state variables can be substituted with their expected steady-state values [4]. Taking into account this statement, (31) is investigated as an example. By using the equations $I_L = V_{ref}/R$ and $V_{0(SS)} = V_{ref}$, the inequality in (31) can be rewritten as follows:

$$\underbrace{\frac{-E_{(\min)}}{\mathrm{LC}} < -\frac{1}{\mathrm{LC}}\left(V_{0(\mathrm{SS})}\right) + \left(\lambda + \beta\gamma\underbrace{\left|V_{0(\mathrm{SS})}^{\gamma-1} - V_{\mathrm{ref}}\right|}_{0} - \frac{1}{R_{(\min)}C}\right)\underbrace{\left(\frac{V_{0(\mathrm{SS})}}{R_{(\min)}C} - \frac{V_{0(\mathrm{SS})}}{R_{(\min)}C}\right)}_{0} < 0}_{\frac{-E_{(\min)}}{\mathrm{LC}} < -\frac{1}{\mathrm{LC}}\left(V_{0(\mathrm{SS})}\right) < 0}. \tag{43}$$

It is extremely clear from equation (43) that any value of coefficients can be chosen for the proposed strategy. The same procedure is followed for the stability analysis, and the coefficients to be chosen are more precisely determined. The control parameters are set to $\lambda = 3600$, $\beta = 10$, $\gamma = 0.2$.

*4.2. Determination of FCL Parameter.* Equation (17) produces a series of $k$th switching periods $(k > 0)$ that correspond to

$$T_k = T_k^+ + T_k^- = 2\Delta\left(p_k^+ - p_k^-\right), \tag{44}$$

where $p_k^+$ and $p_k^-$ are the inverse of (19) and (20), respectively, and $T_k$ is the switching period. The obtaining of (44) relies on the assumption of piecewise linear behavior for $\dot{S}_{\mathrm{FTSMC}}$, which implies that $p_k^+$ and $p_k^-$ remain constant during the switching interval. The $k$th switching period is given as follows:

$$\begin{aligned} T_k = T_k^+ + T_k^- &= p_k^+\left(\Delta_k + \Delta_{k-1}\right) - 2p_k^-\Delta_k = \widehat{p}_k\Delta_k \\ &\quad + \left(\widetilde{p}_k - \widehat{p}_k\right)\Delta_{k-1}, \end{aligned} \tag{45}$$

where $\widehat{p}_k = p_k^+ - 2p_k^-$ and $\widetilde{p}_k = 2\left(p_k^+ - p_k^-\right)$. Switching period error is defined as $e = \mathrm{Ts\_ref} - T_s$. By using (45), it is simple to discover that

$$\begin{aligned} e_k - e_{k-1} &= \widehat{p}_k\left(\Delta_{k-1} - \Delta_k\right) + p_{k-1}^+\left(\Delta_{k-2} - \Delta_{k-1}\right) \\ &\quad + \left(\widetilde{p}_{k-1} - \widetilde{p}_k\right)\Delta_{k-1}. \end{aligned} \tag{46}$$

During controlling the buck converter, the reference value is constant, i.e., it is time-invariant. The steady-state vector can be considered also constant by assuming that the amplitude of the ripple, $2\Delta$, of $S_{\mathrm{FTSMC}}$ in the vicinity of $S_{\mathrm{FTSMC}} = 0$ is small. As a result, the derivatives of the switching function and their inverses are constant in the steady state as well. Consequently, from a certain discrete-time instant $k_0$, it follows that

$$\begin{aligned} p_k^{\pm} &= p\left(V_{\mathrm{ref}}, u \pm\right) = p_*^{\pm}, \\ \widehat{p}_k &= \widehat{p}_k^*, \\ \widetilde{p}_k &= \widetilde{p}_k^*, \quad \forall k \geq k_0, \end{aligned} \tag{47}$$

with $p_*^+, \widehat{p}^*, \widetilde{p}^* \in R^+$ and $p_*^- \in R^-$. With the approximations in (47), the switching period error equation in (46) can be rewritten as follows:

$$e_k - e_{k-1} = \widehat{p}^*\left(\Delta_{k-1} - \Delta_k\right) + p_*^+\left(\Delta_{k-2} - \Delta_{k-1}\right). \tag{48}$$

The proposed control law for the hysteresis band amplitude in the case of a time-invariant reference value is an integral type and yields the following difference equation:

$$\Delta_k = \Delta_{k-1} + \eta e_{k-1}, \tag{49}$$

where $\eta > 0$ referring the integral constant. For stability analysis of FCL, Reference 38 can be visited. In order to ensure that the switching frequency control loop performs consistently within all operating ranges, the value of $\eta$ must be chosen carefully. If the integral gain $\eta$ is selected as

$$0 < \eta < \min\left\{\left(p_*^+\right)^{-1}, \left|p_*^-\right|^{-1}\right\}, \tag{50}$$

then the switching period converges asymptotically to its reference value in the steady state. As can be seen from (50), $p_*^+$ and $p_*^-$ have to be calculated in order to determine $\eta$.

The steady-state values of (18) can be written as follows:

$$\dot{S}_{\mathrm{FTSMC}} = \frac{1}{\mathrm{LC}}\left(uE - V_{\mathrm{ref}}\right). \tag{51}$$

Inverse of (51) for ON and OFF states is found as (52) and (53), respectively.

$$p_*^+ \frac{1}{\left(\dot{S}_{\mathrm{FTSMC}}\right)^+} = \frac{\mathrm{LC}}{E - V_{\mathrm{ref}}}, \tag{52}$$

$$p_*^+ = \frac{1}{\left(\dot{S}_{\mathrm{FTSMC}}\right)^-} = \frac{\mathrm{LC}}{-V_{\mathrm{ref}}}. \tag{53}$$

With the specifications given in Table 1 and taking into account (50), the intervals for integral constant $\eta$ can be found as follows:

$$\left(E, V_{\mathrm{ref}}\right) = (15V, 12V) \longrightarrow \min\left\{\left(p_*^+ = 3.33.10^{-7}\right)^{-1}; \left|p_*^- = -8.33.10^{-8}\right|^{-1}\right\} \longrightarrow \eta < 3003003, \tag{54}$$

$$\left(E, V_{\mathrm{ref}}\right) = (25V, 12V) \longrightarrow \min\left\{\left(p_*^+ = 7.69.10^{-8}\right)^{-1}; \left|p_*^- = -8.33.10^{-8}\right|^{-1}\right\} \longrightarrow \eta < 12004801, \tag{55}$$

$$\left(E, V_{\mathrm{ref}}\right) = (15V, 7V) \longrightarrow \min\left\{\left(p_*^+ = 1.25.10^{-7}\right)^{-1}; \left|p_*^- = -1.43.10^{-7}\right|^{-1}\right\} \longrightarrow \eta < 6993006. \tag{56}$$

Based on the above inequalities, $\eta$ can be chosen between $0 < \eta < 3003003$. To determine the impact of the FCL integral constant value ($\eta$) on switching frequency and other system variables, various simulations have been performed. From Figure 10, a dynamic response with a shorter settling time for the switching frequency is more likely to be obtained with the bigger value of the integral constant. However, the larger $\eta$ causes much more oscillation after the settling of the system as can be seen from the same figure. Once more, a higher $\eta$ can exhibit better robustness against disturbance as shown in Figure 11(a). On the other hand, despite the fact that the inductor current does not need to be measured due to the sliding surface being used, it should still be taken into consideration. Because of the $\Delta IL = (1 - D)V_0/Lf_s$, the ripple in inductor current unfortunately will rise since the bigger $\eta$ produces more oscillation as illustrated in Figure 11(b). Based on the above reasoning and demonstrations, it is inferred that FCL integral constant must be selected with care in order to maintain a balance between switching frequency and inductor current ripple. In study, the integral gain is selected as $\eta = 500$.

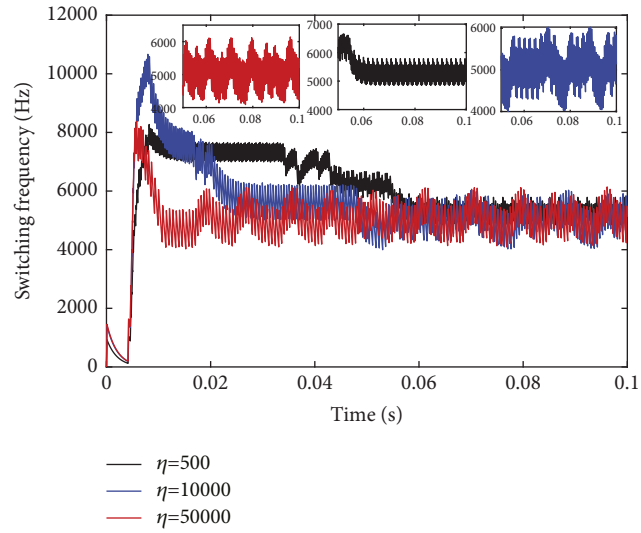


Figure 10: The effect of the FCL integral constant to the switching frequency.

*4.3. Experimental Results under Disturbances and Uncertainties.* The effectiveness of the proposed method is investigated under different operational conditions such as variations in load resistance, input voltage, reference voltage, and the parametric uncertainty in capacitor and inductor values.

*4.3.1. Scenario A-Load Resistance Variation.* Figure 12 depicts the suggested controller's dynamic reactions with and without FCL. In this scenario, the ability to regulate the output voltage of the proposed controller is evaluated by decreasing the load resistance from 10 Ω to 5 Ω. Clearly, the output current is increased from 1.2 A to 2.4 A after the step change. The experimental results show that the proposed control strategy successfully regulates the output voltage to its reference (12 V) against the step change in load resistance. Moreover, before and after the step change, the result reveals that the proposed method is also capable to regulate the output voltage in steady state. In the preceding sections, the switching frequency was calculated theoretically while ignoring the error variables in the steady state, yielding an equation not dependent on load resistance. From a practical point of view, the step change in load resistance may affect the switching frequency. As can be seen from both figures, the load change has only a minor effect on the switching frequency.

*4.3.2. Scenario B-Input Voltage Variation.* Figure 13 illustrates the performance of the modified FTSMC and FCL controllers under a wide range variation in input voltage. In this scenario, the input voltage is increased from 15 V to 25 V and then returns back to the first value. As expected, the FTSMC yields an insensitive behavior under the transient condition regardless of increasing or decreasing the input voltage in both figures. On the other hand, as can be seen from Figure 13(a), when the input voltage is increased, the switching frequency is approximately doubled which means more losses in the converter will arise. Similarly, the switching frequency returns back to the initial level when the input voltage is reduced. These two situations demonstrate that the switching frequency is not in a position to operate in a consistent manner owing to large variations. However, by using FCL, the variations of switching frequency are limited and ensured that the switching frequency remained at the predetermined level as can be observed in Figure 13(b). FCL keeps the frequency constant by changing the hysteresis band adaptively as shown in Figure 13(b).

*4.3.3. Scenario C-Reference Voltage Variation.* This scenario is conducted by changing the reference voltage from 12 V to 7 V and then return to 12 V again. As clearly seen in the Figure 14(a), the output voltage is regulated to its new reference with the help of proposed strategy. In other respects, from Figure 14(a), the switching frequency has a wide range of variations when reference voltage is changed. Unfortunately, this also will adversely affect the operation of the converter. By implementing the FCL control algorithm, it is possible to eliminate such aforementioned problems. As it is seen from Figure 14(a), FCL successfully controls the switching frequency before and after step change.

*4.3.4. Scenario D-Parameter Variation.* Figure 15 demonstrates the effects of variations in the inductance ($L$) and capacitance ($C$) on system performance. The inductance is reduced from 1 mH to 0.7 mH, and the system responses are given in Figure 15(a). As seen from the figure, the proposed voltage controller successfully keeps the output voltage at the desired value against 30% change in inductance. As it seen from (24), the inductance value affects the switching frequency as well. With the help of FCL, the switching frequency is shielded from this uncertainty as illustrated in

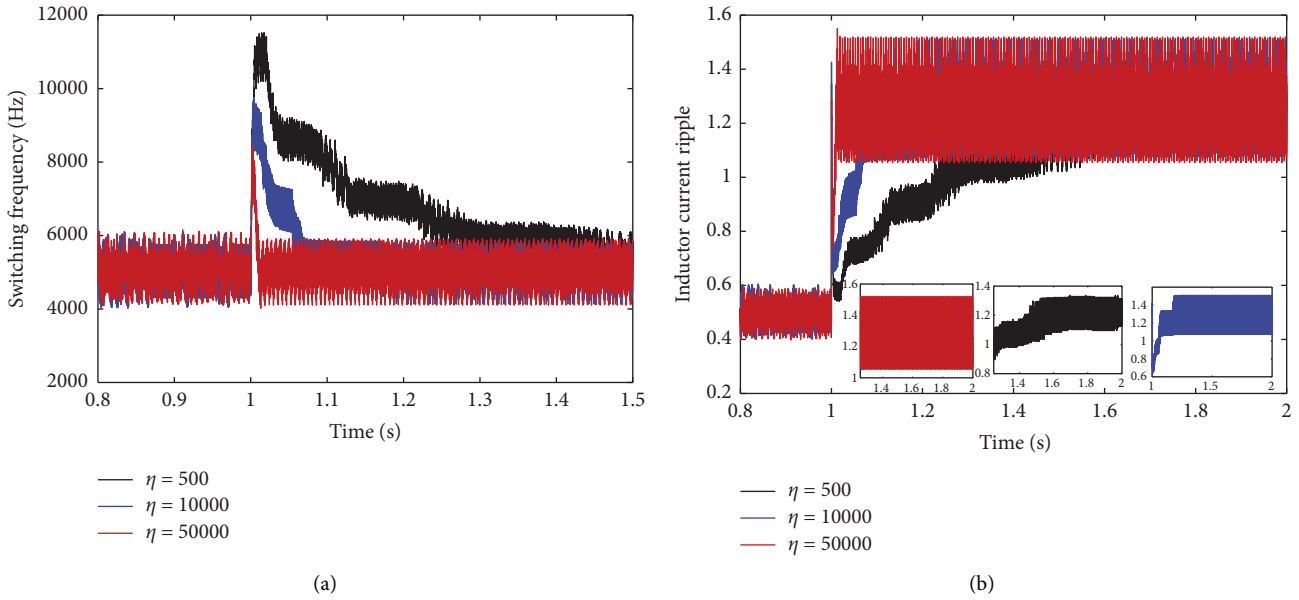


(a) (b)

Figure 11: The effect of the FCL integral constant to (a) the switching frequency during input voltage step change; (b) inductor current ripple during step change of input voltage.

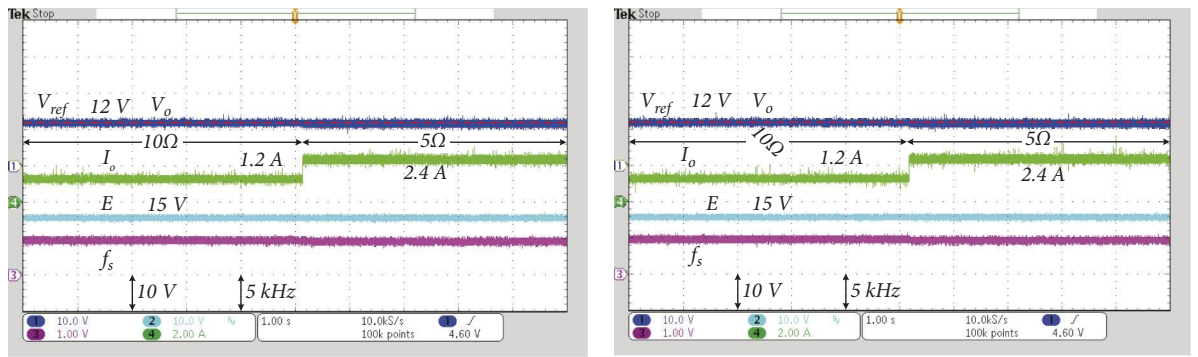


(a) (b)

Figure 12: Proposed control: (a) without FCL; (b) with FCL.

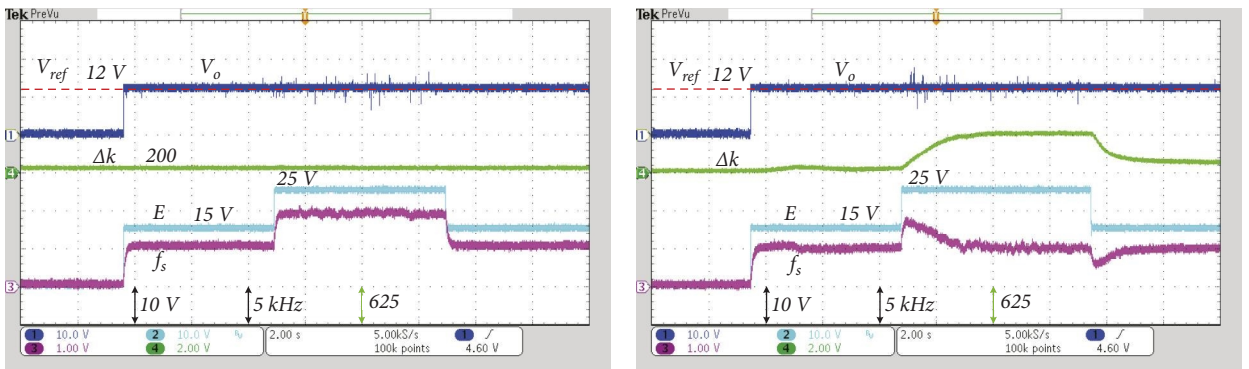


(a) (b)

Figure 13: Proposed control: (a) without FCL; (b) with FCL.

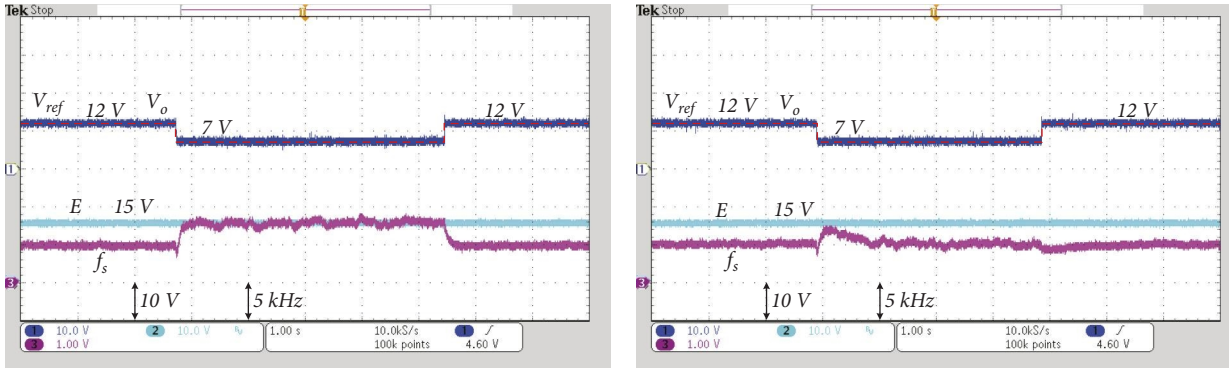


(a) (b)

Figure 14: Proposed control: (a) without FCL; (b) with FCL.

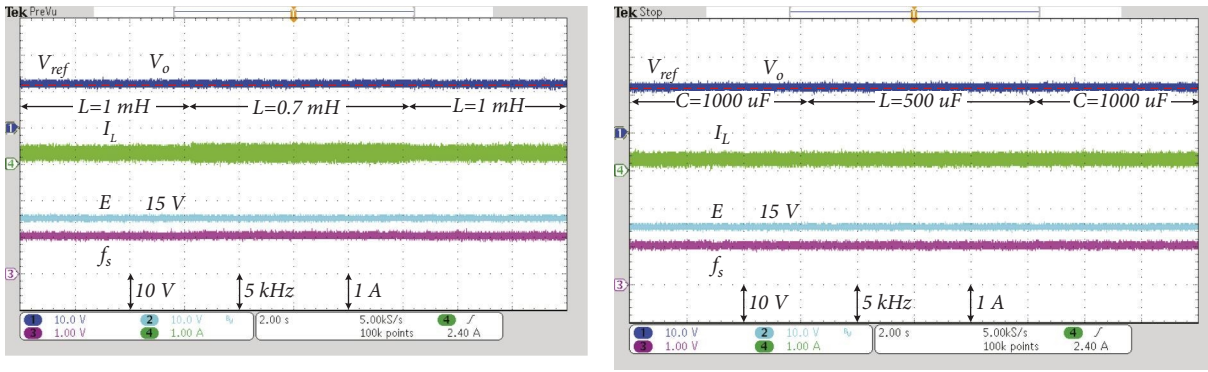


(a) (b)

Figure 15: Proposed controllers against (a) uncertainty in inductor; (b) uncertainty in capacitor.

Table 2: Comparison of four studies with proposed control method from various perspectives.

| Ref | **10** | **16** | **21** | **23** | This paper |
|---|---|---|---|---|---|
| Converter type | Buck | Boost | Buck | Buck | Buck |
| Control strategy | Modified SMC | Modified FTSMC | TSMC | Nonsingular TSMC | Modified FTSMC |
| Number of control parameters $(\lambda, \beta, \gamma)$ | 2 $(\lambda, \beta)$ | 3 $(\lambda, \beta, \gamma)$ | 2 $(\lambda, \gamma)$ | 2 $(\lambda, \gamma)$ | 3 $(\lambda, \beta, \gamma)$ |
| Number of state variables used in $S$ | 2 | 2 | 2 | 2 | 2 |
| Number of sliding coefficients used in $S(\lambda, \beta)$ | 2 $(\lambda, \beta)$ | 2 $(\lambda, \beta)$ | 1 $(\lambda)$ | 1 $(\lambda)$ | 2 $(\lambda, \beta)$ |
| Required sensor | 2 $(I_C, V_0)$ | 2 $(E, V_0)$ | 3 $(I_C, V_0, I_0)$ | 2 $(I_C, V_0)$ | 1 $(V_0)$ |
| Hardware space requirements | Much | Much | So much | Much | Less |
| Variable switching frequency | Exist | Exist | Exist | Exist | Solved |

Figure 15(a). However, because of the relation of $\Delta IL = (1 - D)V_0/Lf_s$, as inductor size is decreased, the inductor current ripple increases as it observed from the figure. The other parametric variation was created by halving the value of the capacitor. From Figure 15(b), the output voltage and switching frequency maintained its response without any change. The findings above reveal that the proposed voltage control method and FCL are robust against parametric disturbances.

For further verification of the effectiveness of modified FTSMC, comparison with four existing studies is presented in Table 2. As can be observed in Table, some of the studies have fewer control parameters than this study, implying that fine-tuning control parameters are easier for them. Contrary to these studies including 16, the proposed study requires only one sensor for control, and thus, the system is less affected by sensor characteristics such as sensitivity, response time, and linearity. Moreover, three other studies

involve the measurement of capacitor current $I_C$ which leads to distortion in capacitor voltage as discussed in [46]. Consequently, the proposed method is more beneficial in terms of eliminating high frequency noises, reliability, cost of the control system, and maintenance requirements.

## 5. Conclusion

In this paper, a modified FTSMC is proposed for DC-DC buck converters. The output voltage of the converter is regulated to its reference by the proposed control strategy. In addition, the switching frequency control method is integrated into the modified FTSMC method. The performance of the proposed control method was investigated in steady-state and transient conditions such as variation in load resistance, input voltage, and reference of output voltage. The proposed control method exhibits good steady-state and transient responses. Also, the experimental results obtained with and without a switching frequency controller loop reveal that high deviations occur in switching frequency in transient cases. The combination of the proposed FTSMC and FCL methods successfully fixes the switching frequency to the desired value. In addition, a further comparison has been done between modified FTSMC and other studies in literature in terms of experimental feasibility. Since the proposed control method needs only one voltage sensor, it presents an easy implementation.

## Abbreviations

$C$: Capacitor
CSMC: Conventional sliding mode control
$\Delta$: (Delta) hysteresis bandwidth
$D$: Diode
$E$: DC input voltage source
$e$: Switching period error
$\eta$: (Eta), integral constant
FTSMC: Fast terminal sliding mode control
FCL: Frequency control loop
HM: Hysteresis modulation
$I_C$: Capacitor current
$I_L$: Inductor current
$I_0$: Load current
$L$: Inductor
$\lambda$: (Lambda)
$\beta$: (Beta)
$\gamma$: (Gamma).

### *Sliding Mode Control Coefficients*

$p_k$: Inverse of $\dot{S}$
$R$: Load resistor
$S$: Sliding surface function
$\dot{S}$: Derivative of $S$
SMC: Sliding mode control
$S_w$: Switch
$T_k$: Switching period
TSMC: Terminal sliding mode control
$u$: Control input
$V_0$: Output voltage
$\dot{V}_0$: Derivative of output voltage
$V_{\text{ref}}$: Output voltage reference
$x_1$: Output voltage error
$\dot{x}_1$: Derivative of output voltage error
$\dot{x}_2$: Derivative of $x_2$.

## Data Availability

The data used to support the findings of this study are available from the corresponding author upon request.

## Conflicts of Interest

The authors declare that they have no conflicts of interest.

## References

[1] D. Cortés, J. Alvarez, and J. Alvarez-Gallegos, "Feedforward and feedback robust control of the buck converter," in *Proceedings of the 15th IFAC World Congress*, Barcelona, Spain, July 21, 2002.

[2] J. Rodriguez and P. Cortes, *Predictive Control of Power Converters and Electrical Drives*, John Wiley & Sons, Chichester, UK, 2012.

[3] Z. Wang, S. Li, and Q. Li, "Discrete-time fast terminal sliding mode control design for dc–dc buck converters with mismatched disturbances," *IEEE Transactions on Industrial Informatics*, vol. 16, no. 2, pp. 1204–1213, 2020.

[4] S. Tan, Y. Lai, and C. Tse, *Sliding Mode Control of Switching Power Converters: Techniques and Implementation*, CRC Press, Boca Raton, FL, USA, 2011.

[5] M. Ahmed, *Sliding Mode Control for Switched Mode Power Supplies. PhD Thesis*, Lappeenranta University of Technology, Finland, Europe, 2004.

[6] M. H. Rashid, *Power Electronics Handbook*, Butterworth-Heinemann, Oxford, UK, 2012.

[7] S. Dhawan, D. Lynn, M. Weber, H. Neal, R. Sumner, and R. Weber, "Ideas on DC-DC converters for delivery of low voltage and high currents for the SLHC/ILC detector electronics in magnetic field and radiation environments," in *Proceedings of the 12th Workshop on Electronics for LHC and Future Experiments (LECC 2006)*, Valencia, Spain, September 2006.

[8] S. Chander, P. Agarwal, and I. Gupta, "Auto-tuned, discrete PID controller for DC-DC converter for fast transient response," in *Proceedings of the India International Conference on Power Electronics 2010 (IICPE2010)*, New Delhi, India, January 2006.

[9] T. K. Nizami, A. Chakravarty, and C. Mahanta, "Analysis and experimental investigation into a finite time current observer based adaptive backstepping control of buck converters," *Journal of the Franklin Institute*, vol. 355, no. 12, pp. 4996–5017, 2018.

[10] B. Naik and A. Mehta, "Sliding mode controller with modified sliding function for DC-DC Buck Converter," *ISA Transactions*, vol. 70, pp. 279–287, 2017.

[11] M. S. Rahman, *Buck Converter Design Issues. Master's Thesis*, Linkoping Institute of Technology, Linköping, Sweden, 2007.

[12] S. Abdelmalek, A. Dali, A. Bakdi, and M. Bettayeb, "Design and experimental implementation of a new robust observer-based nonlinear controller for DC-DC buck converters," *Energy*, vol. 213, Article ID 118816, 2020.

[13] S. Iturriaga-Medina, P. Martinez-Rodriguez, M. Juarez-Balderas, J. Sosa, and C. Limones, "Buck converter controller design in an electronic drive for LED lighting applications," in *Proceedings of the 2015 IEEE International Autumn Meeting on Power, Electronics and Computing (ROPEC)*, Ixtapa, Mexico, November 2007.

[14] F. Bayat, M. Karimi, and A. Taheri, "Robust output regulation of zeta converter with load/input variations: LMI approach," *Control Engineering Practice*, vol. 84, pp. 102–111, 2019.

[15] T. K. Nizami, A. Chakravarty, and C. Mahanta, "Time bound online uncertainty estimation based adaptive control design for DC-DC buck converters with experimental validation," *IFAC Journal of Systems and Control*, vol. 15, Article ID 100127, 2021.

[16] I. Yazici and E. K. Yaylaci, "Fast and robust voltage control of DC-DC boost converter by using fast terminal sliding mode controller," *IET Power Electronics*, vol. 9, no. 1, pp. 120–125, 2016.

[17] A. Derdiyok and M. Levent, "Sliding mode control of a bioreactor," *Korean Journal of Chemical Engineering*, vol. 17, no. 6, pp. 619–624, 2000.

[18] A. Dumlu and K. K. Ayten, "A combined control approach for industrial process systems using feed-forward and adaptive action based on second order sliding mode controller design," *Transactions of the Institute of Measurement and Control*, vol. 41, no. 4, pp. 1160–1171, 2019.

[19] T. K. Nizami, A. Chakravarty, and C. Mahanta, "Design and implementation of a neuro-adaptive backstepping controller for buck converter fed PMDC-motor," *Control Engineering Practice*, vol. 58, pp. 78–87, 2017.

[20] C. Elmas, O. Deperlioglu, and H. H. Sayan, "Adaptive fuzzy logic controller for DC-DC converters," *Expert Systems with Applications*, vol. 36, no. 2, pp. 1540–1548, 2009.

[21] H. Komurcugil, "Adaptive terminal sliding-mode control strategy for DC-DC buck converters," *ISA Transactions*, vol. 51, no. 6, pp. 673–681, 2012.

[22] S. C. Tan, Y. M. Lai, M. K. Cheung, and C. K. Tse, "On the practical design of a sliding mode voltage controlled buck converter," *IEEE Transactions on Power Electronics*, vol. 20, no. 2, pp. 425–437, 2005.

[23] H. Komurcugil, "Non-singular terminal sliding-mode control of DC-DC buck converters," *Control Engineering Practice*, vol. 21, no. 3, pp. 321–332, 2013.

[24] S. C. Tan, Y. Lai, C. K. Tse, and M. K. Cheung, "Adaptive feedforward and feedback control schemes for sliding mode controlled power converters," *IEEE Transactions on Power Electronics*, vol. 21, no. 1, pp. 182–192, 2006.

[25] H. Komurcugil, "Sliding mode control strategy with maximized existence region for DC-DC buck converters," *International Transactions on Electrical Energy Systems*, vol. 31, no. 3, Article ID e12764, 2021.

[26] A. Dehghanzadeh, G. Farahani, H. Vahedi, and K. Al-Haddad, "Model predictive control design for DC-DC converters applied to a photovoltaic system," *International Journal of Electrical Power & Energy Systems*, vol. 103, pp. 537–544, 2018.

[27] R. Silva-Ortigoza, V. M. Hernández-Guzmán, M. Antonio-Cruz, and D. Munoz-Carrillo, "DC/DC buck power converter as a smooth starter for a DC motor based on a hierarchical control," *IEEE Transactions on Power Electronics*, vol. 30, no. 2, pp. 1076–1084, 2015.

[28] M. C. Di Piazza, M. Pucci, A. Ragusa, and G. Vitale, "Analytical versus neural real-time simulation of a photovoltaic generator based on a DC-DC converter," *IEEE Transactions on Industry Applications*, vol. 46, no. 6, pp. 2501–2510, 2010.

[29] V. Utkin, J. Guldner, and J. Shi, *Sliding Mode Control in Electro-Mechanical Systems*, Taylor & Francis, London, UK, 2017.

[30] Y. Wang, H. Xia, and Y. Cao, "Voltage controller of DC-DC buck converter using terminal sliding mode," in *Proceedings of the IECON 2015-41st Annual Conference of the IEEE Industrial Electronics Society*, Yokohama, Japan, November 2015.

[31] H. Du, X. Chen, G. Wen, X. Yu, and J. Lü, "Discrete-time fast terminal sliding mode control for permanent magnet linear motor," *IEEE Transactions on Industrial Electronics*, vol. 65, no. 12, pp. 9916–9927, 2018.

[32] S. K. Gudey and R. Gupta, "Recursive fast terminal sliding mode control in voltage source inverter for a low-voltage microgrid system," *IET Generation, Transmission & Distribution*, vol. 10, no. 7, pp. 1536–1543, 2016.

[33] E. Heydari, A. Y. Varjani, and D. Diallo, "Fast terminal sliding mode control-based direct power control for single-stage single-phase PV system," *Control Engineering Practice*, vol. 104, Article ID 104635, 2020.

[34] S. S. D. Xu, C. C. Chen, and Z. L. Wu, "Study of nonsingular fast terminal sliding-mode fault-tolerant control," *IEEE Transactions on Industrial Electronics*, vol. 62, no. 6, pp. 1–3913, 2015.

[35] S. Yu, X. Yu, B. Shirinzadeh, and Z. Man, "Continuous finite-time control for robotic manipulators with terminal sliding mode," *Automatica*, vol. 41, no. 11, pp. 1957–1964, 2005.

[36] C. U. Solis, J. B. Clempner, and A. S. Poznyak, "Fast terminal sliding-mode control with an integral filter applied to a van der pol oscillator," *IEEE Transactions on Industrial Electronics*, vol. 64, no. 7, pp. 5622–5628, 2017.

[37] X. Yu and M. Zhihong, "Fast terminal sliding-mode control design for nonlinear dynamical systems," *IEEE Transactions on Circuits and Systems I: Fundamental Theory and Applications*, vol. 49, no. 2, pp. 261–264, 2002.

[38] V. Repecho, D. Biel, J. M. Olm, and E. F. Colet, "Switching frequency regulation in sliding mode control by a hysteresis band controller," *IEEE Transactions on Power Electronics*, vol. 32, no. 2, pp. 1557–1569, 2017.

[39] H. Komurcugil, S. Biricik, S. Bayhan, and Z. Zhang, "Sliding mode control: overview of its applications in power converters," *IEEE Industrial Electronics Magazine*, vol. 23, no. 2, pp. 746–753, 2014.

[40] A. Goudarzian, A. Khosravi, and N. R. Abjadi, "Sliding mode current control of a NOCULL converter based on hysteresis modulation method in a wide range of operating conditions," *ISA Transactions*, vol. 85, pp. 214–225, 2019.

[41] P. Mattavelli, L. Rossetto, G. Spiazzi, and P. Tenti, "General-purpose sliding-mode controller for DC/DC converter applications," in *Proceedings of IEEE Power Electronics Specialist Conference-Pesc'93*, pp. 609–615, Seattle, WA, USA, June 1993.

[42] R. Guzman, L. G. De Vicuna, J. Morales, M. Castilla, and J. Matas, "Sliding-mode control for a three-phase unity power factor rectifier operating at fixed switching frequency," *IEEE Transactions on Power Electronics*, vol. 31, no. 1, pp. 758–769, 2016.

[43] D. G. Holmes, R. Davoodnezhad, and B. P. McGrath, "An improved three-phase variable-band hysteresis current regulator," *IEEE Transactions on Power Electronics*, vol. 28, no. 1, pp. 441–450, 2013.

[44] J. M. Ruiz, S. Lorenzo, I. Lobo, and J. Amigo, "Minimal UPS structure with sliding mode control and adaptive hysteresis band," in *Proceedings of the IECON'90: 16th Annual*

*Conference of IEEE Industrial Electronics Society*, Pacific Grove, CA, USA, November 1990.

[45] R. R. Ramos, D. Biel, E. Fossas, and F. Guinjoan, "A fixed-frequency quasi-sliding control algorithm: application to power inverters design by means of FPGA implementation," *IEEE Transactions on Power Electronics*, vol. 18, no. 1, pp. 344–355, 2003.

[46] H. Pang and P. M. Bryan, "A life prediction scheme for electrolytic capacitors in power converters without current sensor," in *Proceedings of the 2010 Twenty-Fifth Annual IEEE Applied Power Electronics Conference and Exposition (APEC)*, Palm Springs, CA, USA, February 2010.